Surfaces, Interfaces, and Catalysis; Physical Properties of Nanomaterials and Materials

Unexpected Optical Blue-Shift in Large Colloidal Quantum Dots by Anionic Migration and Exchange

Maria Acebron, Juan F. Galisteo-López, Cefe Lopez, Facundo C. Herrera, Martin D. Mizrahi, Felix G Requejo, Francisco Javier Palomares, and Beatriz H. Juarez

J. Phys. Chem. Lett., **Just Accepted Manuscript** • Publication Date (Web): 21 May 2018

Unexpected Optical Blue-Shift in Large Colloidal Quantum Dots by Anionic Migration and Exchange

María Acebrón[a], Juan F. Galisteo-López[b], C. López[c], Facundo C. Herrera[d], Martín Mizrahi[d], Félix G. Requejo[d], F. Javier Palomares[c], Beatriz H. Juárez[a,e]

[a] IMDEA Nanoscience, Faraday 9, Cantoblanco, 28049, Madrid, Spain

[b] Instituto de Ciencias de Materiales de Sevilla (ICMS), Consejo Superior de Investigaciones Científicas (CSIC), 41092 Sevilla, Spain

[c] Instituto de Ciencias de Materiales de Madrid (ICMM), Consejo Superior de Investigaciones Científicas (CSIC), 28049, Madrid, Spain

[d] Instituto de Investigaciones Fisicoquímicas Teóricas y Aplicadas (INIFTA), CONICET and FCE, UNLP, CC/16, suc 4, 1900 La Plata, Argentina

[e] Applied Physical Chemistry department, Universidad Autónoma de Madrid, Cantoblanco, 28049, Madrid, Spain

ABSTRACT:

Compositional changes taking place during the synthesis of alloyed CdSeZnS nanocrystals (NCs) allow shifting the optical features to higher energy as the NCs grow. Under certain synthetic conditions, the effect of those changes on the surface/interface chemistry competes with and dominates over the conventional quantum confinement effect in growing NCs. These changes, identified by means of complementary advanced spectroscopic techniques such as XPS (X-ray Photoelectron Spectroscopy) and XAS (X-ray absorption Spectroscopy), are understood in the frame of an ion migration and exchange mechanism taking place during the synthesis. Control over the synthetic routes, during the NCs growth, represents an alternative tool to tune the optical properties of colloidal quantum dots, broadening the versatility of the wet-chemical methods.

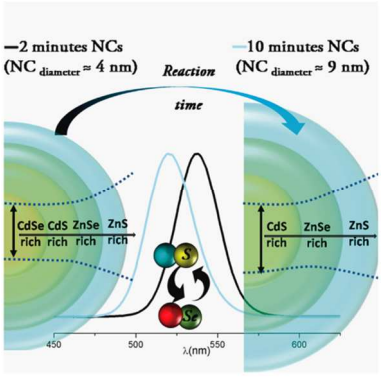

Semiconductor nanocrystals (NCs) have benefited from straightforward wet chemical synthetic methods that provide relatively low-cost, efficient, and high-quality emitting materials.[1] Nowadays, improved control over particle size, shape, composition, crystallinity, and surface chemistry have triggered their applications ranging from flat-screens, to lasers or biological markers.[2, 3] However, these NCs are still the motivation of numerous fundamental physico-chemical studies, being the focus of very active research in the quest for materials with tunable and robust optical and electronic properties.[3-5]

The diversity of synthetic procedures and suitable chemical precursors have led to a broad variety of NCs, most of them showing well-defined optical properties whose evolution is consistent with variations of composition, size or shape, and mainly explained by the quantum confinement effect. While size and composition are the two main factors affecting the optical properties, the spatial distribution of elements, and the nature of the interfaces between the different regions composing the NCs also influence the final optical response. Among these NCs, multinary ones (tertiary or quaternary in composition), are gaining interest in solar power conversion and *in vivo* imaging, where larger wavelength and very stable emission are demanded.[6] Unfortunately, since multiple elemental combinations are possible in these systems, reproducible composition and stoichiometry are still tough tasks, especially when all precursors are included in the synthesis recipient at the same time. In these NCs, the formation of different phases may not only produce the traditional core-shell-like NCs but also graded or alloyed ones with a chemical composition gradient.[7-9] In all these structures the lattice mismatch at the interface between each component plays a critical role in their final optical response and, therefore, in their applicability.[10]

The alloyed structures with a chemical composition gradient possess a smoothed confinement potential and have been recently revealed as robust and efficient systems.[7, 11-15] They can be synthesized by several methods,[13-18] including the use of post-synthetic treatments such as annealing procedures of core-shell NCs produced by hot-injection,[19, 20] or ion exchange processes promoted by the NCs incubation in suitable media.[21-24]

During the injection methods, NCs' composition and optical properties are governed by synthetic parameters, being traditionally explained in terms of the used precursors, solvents, and temperature, which regulate the NCs' nucleation and growth processes. While in these procedures,[13, 14, 16] the composition of the NCs at different reaction times have been widely studied, there is a lack of a detailed explanation of the role of migration and/or exchange of elements on the compositional changes during growth. These mechanisms are well-known and are the basis of the preparation of a broad palette of NCs from previously prepared seeds, either by replacement or addition of ions to the initial

lattice.[19-25] In this work, however, we report on the elucidation of these mechanisms not in previously prepared NCs, but during the growth evolution of quaternary NCs by hot injection.

It will be shown that the synthetic parameters can be programmed not only to control nucleation and growth but also as a tool to tune *in situ* the optical properties of alloyed structures on the basis of ion exchange and migration mechanisms. Subtle changes on precursors feeding during the synthesis of alloyed CdSeZnS allow modulating the NCs' optical response to obtain either the customary red-shift, as previously reported,[15, 16] or an unexpected blue-shift in the optical properties as the NCs grow. In this case, the traditional red-shift concomitant to the increasing NCs' size competes with compositional changes taking place during the reaction. The upshot of this competition is mainly controlled by temperature, which defines the evolution of the NCs' structures and optical properties. Notably, in this work the changes in composition, responsible for the intriguing blue-shifted optical response as the NCs grow larger, have been elucidated through advanced characterization including X-Ray Photoelectron Spectroscopy (XPS), X-Ray Absorption Spectroscopy (XAS), and Time-Resolved Spectroscopy. The results are understood in the frame of ion exchange and migration mechanisms taking place, not after post-treatments, but *in-situ* during the synthesis of the NCs, which provides an extra degree of freedom and increases the versatility of the hot-injection method.

We selected a simple single-injection method to produce CdSeZnS NCs following previously reported procedures with some modifications.[15] Briefly, the Cd and Zn precursors (CdO (0.05 mmol) and Zn stearate (2 mmol), respectively) were placed in a three neck round flask in the presence of oleic acid (OA, 8 mmol) and the mixture was heated up to 150 °C under nitrogen atmosphere. Once this temperature was reached, the solution was degassed under vacuum for 30 minutes. Further, octadecene (ODE, 7.5 ml) was added as reaction media and the temperature was raised to 300 ºC. At this stage, the injection of Se (0.2 mmol) and S (1.5 mmol) precursors in a trioctylphosphine (TOP, 2 mmol) solution was quickly performed. After injection, the temperature was decreased 10 °C, favoring the growth process. Finally, the reaction was quenched using a cold-water bath and the addition of dodecanethiol (DDT, 6 mmol) at 200 ºC. Aliquots at 2 minutes intervals were taken during the first 10 minutes of reaction to investigate the NCs' evolution.

The accepted formation mechanism for these NCs is explained as follows: Cd and Zn precursors in the presence of OA form the cationic complexes Cd-OA and Zn-OA. Separately, by dissolving elemental sulfur and selenium powders in TOP, Se-TOP and S-TOP are formed. Once the injection is performed at high temperature (300 ºC), the nucleation process starts, which will be driven by Cd and Se reaction since their reactivity is higher than that of Zn and S. This fact is explained by the higher binding energy of Zn and S with the surfactants than those of Cd and Se precursors.[8, 16] On the other hand, it has been proved that, at this temperature, the reactivity of Se precursor is higher than that of S, showing a higher consumption of Se during the first stage of the reaction.[8, 16] Similarly, as widely reported, the reactivity of Cd-OA complexes is higher than that of Zn-OA, leading to an earlier Cd consumption and structures with Cd-compounds rich cores.[8, 16] Taking into account this reactivity, the structure of the expected NCs would be similar to the extensively reported alloyed systems in which a CdSe-rich core is surrounded by a ZnS-rich shell.[8, 15, 16] Under this assumption, a type I NC with a CdSe core and a shell with composition gradient from CdS, to ZnSe and, finally, ZnS in the outer part of the shell is predictable. During the NCs growth, the leakage of excitons in the graded shell produces the well-observed and reported red-shift of the optical properties (absorption edge and photoluminescence peak).[16, 26]

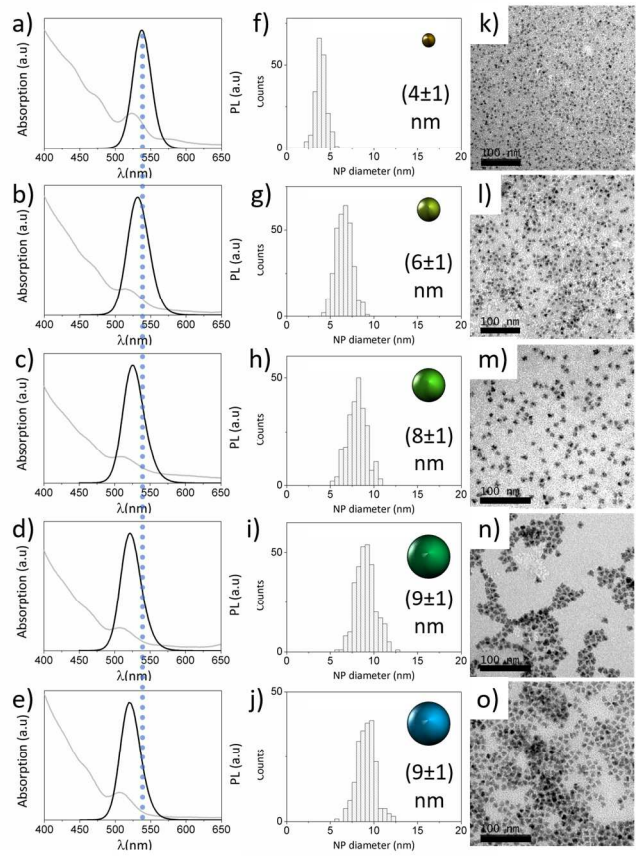

Figure 1. Absorption (gray line) and PL (black line) spectra (a-e) along with size histograms (f-j) and TEM images (k-o) of CdSeZnS NCs grown for 2 (a, f and k), 4 (b, g and l), 6 (c, h and m), 8 (d, i and n), and 10 minutes (e, j and o). Scale bar in TEM images: 100 nm. Spheres in f-j represent the growing NCs whose colors correspond to the emitted PL.

In this work, however, an anomalous evolution of the optical properties is reported for alloyed CdSeZnS NCs. In Figure 1, the absorption and emission spectra of NCs produced after 2, 4, 6, 8 and 10 minutes of reaction (Figure 1a-e) are shown. Their corresponding size histograms (Figures 1f-j) and Transmission Electron Microscopy (TEM) images (Figures 1k-o) were also included in this figure. High Resolution-TEM (HRTEM), and Scanning (STEM) images can be found in the Supporting Information (Figure S1, SI). In Figure 1 it can be observed that the optical properties follow a trend drastically different from that expected for a regular alloyed system with a chemical composition gradient where the absorption edge and the photoluminescence (PL) red-shift with the increasing size.[16, 26] As evidenced, the properties of these NCs are not governed solely by the expected quantum confinement effect, since the bigger the NCs, the more energetic the optical feature (see dotted line in Figures 1a-e) with a mean blue shift of 15 nm.[27]

For a better understanding of the evolution of the optical response Time-Resolved PL measurements were performed to study the NCs´ growth (see Figure S2, SI). The observed decrease in the life time values with reaction time (34.4, 20.3 and 17.3 ns for 2, 4 and 8 minutes NCs, respectively) represents the expected trend to what Fermi's Golden rule predicts for an ideal two-level quantum emitter, that is faster decay times accompanying a blueshifted emission.[28] However while this trend does not correspond to an increased NC size where a reduced quantum confinement is expected, it is in accordance with recent reports for NCs of different nature. For single composition and core-shell systems a similar

trend has been associated with the role of non-radiative processes[29] and for the case of alloyed NCs compositional changes have been shown to drastically modify a given tendency of exciton radiative lifetime with NCs size.[30] Thus, while NC size is well known to affect its optical response, the existence of compositional changes throughout the growth process (see below) will also determine the final properties of the NCs.

To investigate the evolution of the NC´s elemental composition, aliquots of 2 and 10 minutes of reaction were analyzed by XPS, XAS and Total Reflection X-Ray Fluorescence (TXRF). Figure 2 shows the XPS spectra of 2 and 10 minutes NCs (green and red lines, respectively) obtained for the Cd 3d (Figures 2a, 2e and 2g), Zn $2p_{2/3}$ (Figure 2b, 2f and 2h), and Se 3p - S 2p (Figures 2i and 2j) core levels, along with those spectra corresponding to the X-ray Auger electron (XAES) emission from Cd and Zn atoms (Figures 2c and 2d, respectively). Although all these spectra evidence the presence of Cd and Zn sulfides and selenides in both samples,[31, 32] the chemical shift difference of the possible species is very small and an unequivocally assignation to the different contributions is not straightforward. Indeed, a chemical differentiation is unachievable when non-monochromatic radiation is used in the XPS experiments (see SI for further information, Figure S3). Having said that, some differences in terms of line-shape and widths as the reaction proceeds can be readily distinguished when monochromatic Al Kα radiation is applied and high-resolution XPS measurements are performed, as the case here reported

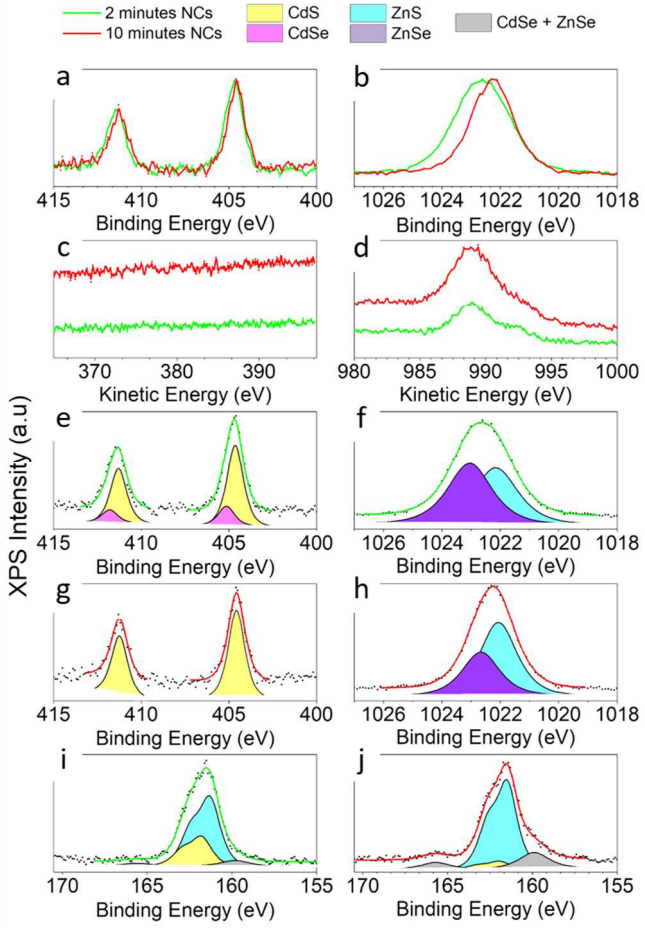

Figure 2. XPS spectra of 2 (green lines) and 10 minutes (red lines) NCs for the Cd 3d (a, e and g) and Zn $2p_{3/2}$ regions (b, f and h). Cd MNN (c) and Zn LMM (d) XAES emissions. Se 3p/S 2p core levels for 2 (i) and 10 minutes (j) NCs.

where species with binding energies separated by less than 0.5 eV can be easily distinguished. Comparing the Cd 3d and Zn $2p_{3/2}$ core levels for the different NCs (Figures 2a and 2b) a modification in the NCs' structure with time is inferred. As shown in Figure 2a and 2b, 2 minutes NCs provide slightly broader signals (green lines) than that of 10 minutes ones (red lines). Indeed, the emission signals provided by 2 minutes NCs display a slight asymmetry on the high binding energy side in both core levels.

Beside the determination of NCs' composition, we can take advantage of the XAES emission to extract farther useful information. On the one hand, the absence of the Cd-MNN transition in both samples (Figure 2c), confirms that the Cd atoms are mainly located at the inner core of the NCs as the low kinetic energy of those Auger electrons allows their detection exclusively when the atoms are located at the outermost layers. On the other hand, the Zn-LMM transition provides chemical information complementary to that of Zn 2p signals, and its line-shape depends on the chemical environments.[33, 34] In this case, the line-shape of Zn-LMM signals recorded for both NCs (Figure 2d) is similar to that of a semiconducting phase such as ZnSe and/or ZnS, discarding the existence of Zn in a metallic state.[33] Indeed, the line-shape of the spectrum after 10 minutes is modified probably due a superposition of two different XAES emissions corresponding to two chemical environments (ZnSe and ZnS).[33, 34] Additionally, as the kinetic energy of the electrons involved in the LMM-transition is high, these signals are emitted from deeper regions and, in this particular case, from all layers throughout the NCs.

Thus, XAES confirms the core-shell-like nature of our NCs and suggests different chemical environments for Zn atoms depending on the reaction time. The curve fitting of the different core levels for both NCs allow the accurate chemical identification of the different species. As shown in Figures 2e and 2f, for 2 minutes NCs two symmetric components with FWHM values similar to those previously reported elsewhere[34-36] are required to properly fit both Cd and Zn core levels. After 10 minutes of reaction a single contribution provides a reasonable fit for the Cd 3d spectrum (Figure 2g) while two components are needed to appropriately fit the Zn $2p_{3/2}$ spectrum (Figure 2h). As shown by these results, as the reaction evolves, the number of Cd species is reduced while Zn atoms maintain their chemical environments. Comparing the obtained results with previously reported ones, [32, 36-38] the contribution at high binding energy values (pink and violet solid areas) could be ascribed to Cd and Zn selenides (CdSe and ZnSe, respectively) while the others (yellow and blue solid areas) are related to sulfides (CdS and ZnS, respectively). According to this assignation, after 10 minutes of reaction the existence of CdSe is discarded while CdS is currently detected. This behavior points to a reduction in the Cd species diversity by the migration and exchange of ions, although disordered regions with defect-like bonding expected in the outer surface of the 2 minutes NCs might also contribute to the spectral modification.

In addition, in the Zn $2p_{3/2}$ spectra it is observed that the ratio of ZnSe to ZnS is decreased after 10 minutes of reaction (Figures 2f and 2h), suggesting a thicker layer of ZnS in 10 minutes NCs and supporting the observed increasing NCs' size. These features are also in accordance with the results shown for Se 3p and S 2p core levels (Figures 2i and 2j) where two different contributions were required to properly fit both S 2p spectra and the ratio between both sulfides change with time. As shown in Figure 2j, although both CdS and ZnS are detected, a thick layer of ZnS after 10 minutes of reaction is confirmed again. Finally, in these figures it can be observed that the contribution of Se 3p to these spectra is increased after 10 minutes of reaction, (grey solid areas), once more supporting the increasing NCs' size observed by TEM. For comparison, the spectra of the Se 3d region for both 2 and 10

minutes NCs can be seen in Figure S3, SI. It is worth mentioning that, although a qualitative analysis of the results is allowed, the direct quantitative comparison of the contents between the two samples is not possible. The different NCs size and subsequent surface-to-volume ratio define different density of ligands at the NCs surface which can cover-up the real intensity of XPS signals.

To complete and complement the structure elucidation in the whole NCs volume, XAS characterization was performed using synchrotron radiation at SXS and XAFS2 beamlines of LNLS (Campinas, Brazil). In particular, X-ray Absorption Near Edge Structure (XANES) spectra for 2 and 10 minutes NCs were recorded, some of them included in Figure 3, where the spectra for aliquots and reference compounds (CdSe NCs, ZnS and ZnSe) at the Zn K-edge and at the Se K-edge are shown (Figure 3a and 3b, respectively). Additional XANES spectra at the S K- and Cd L_3-edges along with further experimental details can be found in the Supporting Information (see Figure S4). Inspecting the XANES spectra taken at the Zn K-edge, ZnS and/or ZnSe seem to be present in both samples. Meanwhile, the results obtained at Se K-edge, suggest that our samples are slightly more similar to the ZnSe reference compound, although the presence of CdSe cannot be completely ruled out. Complementarily, comparing XANES results obtained at the S K- and Cd L_3-edges (SI, Figure S4) with information of several standards and samples reported in the literature,[39-43] multiple combinations of elements are feasible. Indeed, from the Cd L_3-edge (Figure S4a, SI), since both CdSe or CdS compounds present similar spectra,[40, 41] a clear identification of species is not straightforward. However, as shown above, XPS experiments allow the chemical differentiation, ruling out the existence of CdSe after 10 minutes of reaction and confirming the presence of ZnS and ZnSe independently of the reaction time. Meanwhile, CdSe is exclusively detected in 2 minutes NCs.

In order to shed light on the NCs structural conformation, Extended X-ray Absorption Fine Structure (EXAFS) measurements were performed at the Zn and Se K-edges. While Zn atoms could be forming ZnS and ZnSe, as it was previously stated by XPS and XANES results, the peak position at the Fourier Transform (FT) of the EXAFS oscillation, at the Zn K-edge shown in Figure 3c, evidences that Zn atoms in both samples must be forming mostly ZnS. This statement also extracted from XPS results is further confirmed by the fits of EXAFS oscillations (see Table S1 at SI), which provide an average coordination number (ACN) for Zn-S of 3.0 and 3.6 for the 2 and 10 minutes NCs samples, respectively. The obtained ACNs are lower than that corresponding to the ZnS reference compound (ACN = 4) indicating that, in our samples, an important fraction of Zn atoms is coordinatively unsaturated, presumably by being on the NCs' surface. In addition, the Zn-S bond distance in both samples is in agreement with the corresponding distance in ZnS (see Table S1, SI).

The direct analysis of the first coordination shell for Se in both samples provides further clarifying information. In Figure 3d, the FT at the Se K-edge EXAFS spectra for the samples and reference compounds (ZnSe and CdSe) are displayed, and, as shown, remarkable differences between both NCs are now revealed. For 2 minutes NCs, the FT at the Se K-edge EXAFS spectrum does not correspond to pure ZnSe or CdSe reference compounds but to a combination of them. This result means that 2 minutes NCs are composed of both CdSe and ZnSe, as reveled by XPS measurements and expected for an alloyed NCs. According to the precursor´s reactivity and XPS results, the Se atoms in these NCs must be composing a CdSe-rich core and a ZnSe-rich shell. For this reason, two coordination shells, one of Zn atoms and other of Cd atoms were fitted, obtaining an ACN of 1.6 Zn atoms and 1.8 Cd atoms (see Table S2 in SI). It is interesting to note that the total coordination number (N_{SeZn}+ N_{SeCd}) is 3.4, lower than that expected for bulk ZnSe (4). This difference can be explained con-

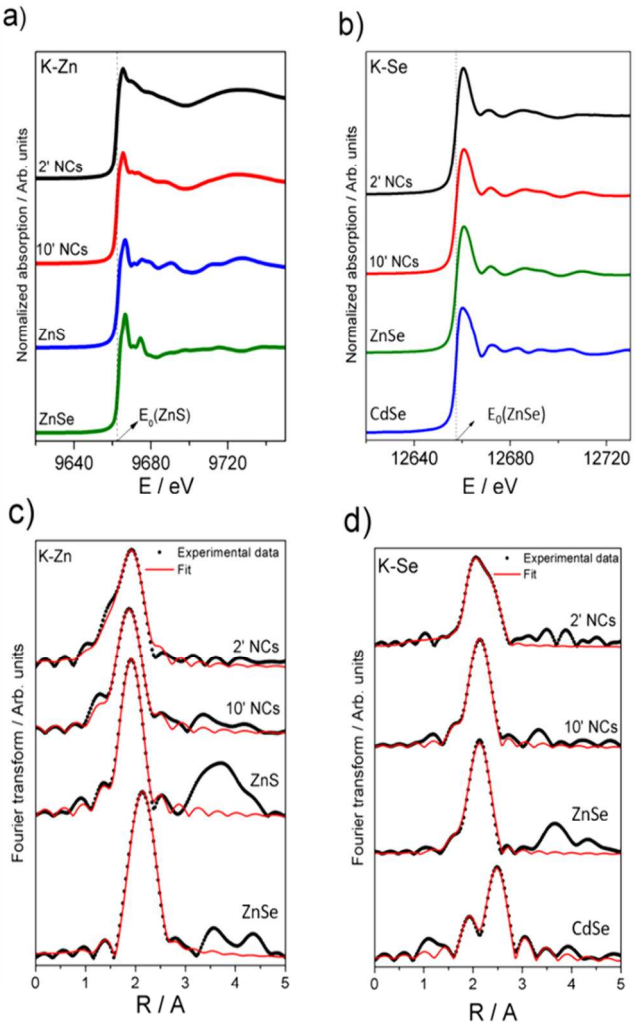

Figure 3. XANES spectra of 2 (black dotted lines) and 10 minutes (red full lines) treated NCs compared with ZnS, ZnSe, SeZn and CdSe reference compounds at the Zn K-edge (a) and Se K-edge (b). Vertical dotted lines in (a) and (b) indicate the energy edge position for ZnS and ZnSe at Zn and Se K-edge, respectively. Fourier transforms of the EXAFS oscillation at the Zn (c) and Se (d) K-edges, for 2 and 10 minutes NCs along with the mentioned reference compounds.

sidering that Zn atoms are at the shell of the NC, and thus the Se atoms forming ZnSe with some of them, contribute to the N_{SeZn} with a lower value than that expected for the inner region. Although the calculation of the percentage of Se atoms coordinated to Zn is not straightforward, it can be estimated about 50%, while the rest are forming an alloy with the Cd at the core of the NC. Indeed, the existence of CdSe at the very begging of the reaction was ascertained by XAS experiments performed on NCs grown for shorter times (0 minutes). Figure S5, SI shows the FT of the EXAFS oscillation for a sample taken a few instants after Se and S precursor injection (0 minutes NCs) compared to 2 and 10 minutes NCs samples (the corresponding fits can be also found in Table S2, SI).

From the FT of 10 minutes NCs (Figure 3d), it is evident that Se is, in this case, exclusively coordinated to Zn atoms forming ZnSe (no CdSe is detected). This asseveration was confirmed by XPS results, but also by the fitted EXAFS results (see Table S2 in SI), where only a first shell of Zn atoms was necessary to perform accurate fits. These fits provide an ACN Se-Zn of 3.9 and an

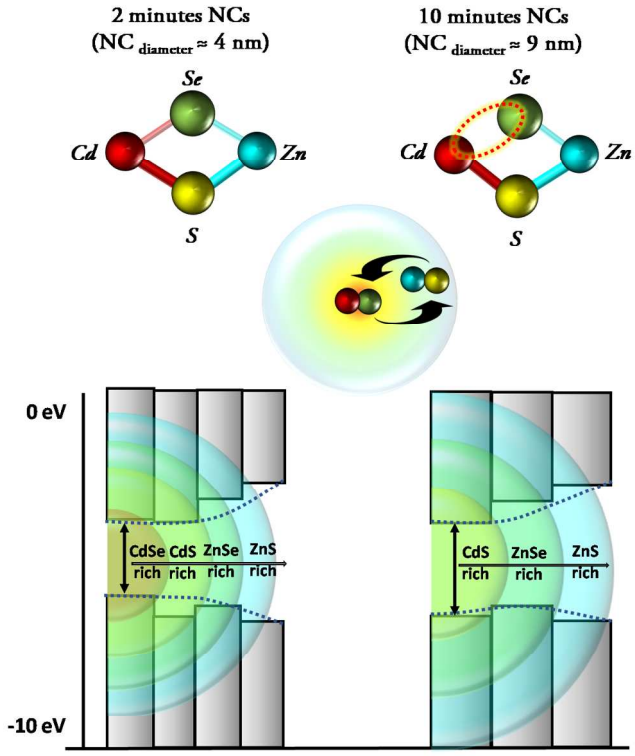

Figure 4. Top: schematical description of element coordination in 2 (left) and 10 minutes (right) NCs. Dotted-line represent the absent Cd-Se bond in 10 minutes NCs. Thick and thin lines represent the major and minor phases, respectively. Middle: Scheme of the ion migration and exchange mechanism, where Se from the core migrates to the outer shell and is exchanged for S. Bottom: proposed energy bandgap diagrams of 2 and 10 minutes NCs.

interatomic distance of 2.45 Å, in accordance with the expected values for ZnSe. It is worth noting that the identification of this ZnSe during the experiments performed at the Zn K-edge, was impossible due to the fact that EXAFS is an average technique over all absorbing atoms and, since the number of Zn and S atoms are much greater than that of Se, the contribution of ZnSe to these spectra cannot be clearly differentiated. This fact emphasizes the importance of using XAS and XPS measurements which are complementary and chemically selective techniques.

The gathered information from XPS, XANES and EXAFS results is schematically depicted in Figure 4 (top) showing that, in both NCs, Zn atoms are shared between S and Se, located at the shell of the NCs forming mainly ZnS, and in a minority fraction ZnSe (notice the thick and thin layers connecting the atoms, representing the major and minor phases present, respectively). Thus, the coordination state of Zn atoms does not suffer drastic modifications as the reaction evolves. In fact, the Se atoms are those whose coordination changes. In the case of 2 minutes NCs, Se atoms are present at the core, coordinated to some Cd atoms, while the rest of the Cd is forming CdS.

Meanwhile, for 10 minutes NCs, no evidence of CdSe was found (see dotted circle in Figure 4, top), with all Se being coordinated exclusively to Zn at the NC surface, being a minority fraction whereas ZnS maintains its dominant contribution. Meanwhile, CdS is the unique phase detected at the NCs' core.

These results indicate that, contrary to an expected CdSe-rich core and a ZnS-rich shell, these NCs suffer a drastic modification on their composition as the reaction proceeds, where the NCs' electronic structure is modulated by a compositional gradient giving rise to alloyed NCs with a CdS-rich core. This modification can be explained in terms of an ion migration and exchange mechanism. In an ion migration scenario, the presence of CdSe after 2 minutes, and its absence 8 minutes later, points to a Se migration from the inner core to the outer shell. Indeed, an indication of this Se migration is evidenced in our current XPS results where a Se-rich surface is detected even for 2 minutes NCs, also in agreement with our previously reported work .[27] To investigate if this ion migration is accompanied by an exchange of elements, NCs produced for 2 and 10 minutes of reaction were further analyzed by TXRF. Table 1 shows the % atomic contents of S, Se, Zn and Cd for 2 and 10 minutes NCs, where significant changes are exclusively observed for Se and Zn, supporting an increased NCs size, as already observed by TEM inspections. As shown, the Cd content is quantitatively consumed after the first 2 minutes of reaction suggesting that the CdS present after 10 minutes must be formed at expenses of the initial CdSe present in 2 minutes NCs and, therefore, an anion exchange mechanism of Se for S is plausible (schematically depicted in Figure 4, middle). It is worth mentioning that this mechanism cannot be extrapolated from the sulfur content values due to the impossibility to distinguish from inorganic S and thiolated ligands. Likewise, cation migration could also contribute to the structures' modification, as similar blue-shifts were observed by the group of Eychmüller,[7] after annealing post-treatments on previously prepared core-shell CdSe-ZnSe NCs and explained in terms of Zn migration to the inner core.[7] We ascertained that in the synthesis reported here the migration must be triggered by the reaction temperature (300 °C), since decreasing it to 260 °C yields the expected red-shift optical properties with increasing NCs' size.[27]

In general, the degree of any ion migration will dictate the final contribution of a particular compound to the NCs volume and thus, influence the final optical properties accordingly. This feature gives idea of the diversity of composition in alloyed NCs. We believe that ion migration and anion exchange mechanisms are responsible for the change in the NCs composition and, as a consequence, in their band-gap structure as schematically depicted at the bottom of Figure 4. According to the evidences presented here, this energy band modification is responsible for the observed blue-shift in the evolution of the optical properties as the CdSe at the inner core is replaced by CdS with larger band-gap.

Table 1. TXRF % atomic contents after 2 and 10 minutes of reaction

Sample	S	Se	Zn	Cd
2 minutes NCs	46.3	2.6	49.7	1.4
10 minutes NCs	36.5	7.3	54.7	1.4

In conclusion, in this work we report on the synthesis and characterization of alloyed CdSeZnS NCs presenting an unexpected blue-shift in their optical properties as the reaction evolves. The use of advanced XPS, XANES and EXAFS techniques provides a very comprehensive study that allows the identification of the variations on NCs composition with time. This structural modification consists on the presence of CdSe in the initial stages of the reaction and its absence after several minutes. These results clarify the feasible mechanisms of ion migration and exchange scenarios dominating the optical response. Moreover, the experiments performed at lower temperatures evidenced that these mechanisms are controllable by this parameter and validate the need of profuse characterization methodologies to fully control the properties of these nanomaterials. In particular, this work provides new insights in the characterization of alloyed NCs through the combination of

XAS and XPS techniques. Further, it demonstrates an additional route to tune the composition of QDs and to modulate the emission wavelength through band-gap engineering.

ASSOCIATED CONTENT

Supporting Information

HRTEM and STEM images of 2 and 8 minutes NCs (Figure S1). Decay dynamics measurements of 2, 4 and 8 minutes NCs (Figure S2). XPS experimental details and XPS spectra for 2 and 10 minutes NCs at the Se 3d region (Figure S3). XAS experiments details, XANES spectra at Cd L_3-edge and S K-edge for 2 and 10 minutes NCs (Figure S4). Fourier transforms of the EXAFS oscillation at the Se K-edges, for 0, 2 and 10 minutes NCs (Figure S5). Fitted Zn and Se K-edges EXAFS results (Tables S1 and S2, respectively).

AUTHOR INFORMATION

Corresponding Author

Beatriz H. Juarez (beatriz.hernandez@uam.es
beatriz.hernadez@imdea.org)

Notes

The authors declare no competing financial interests.

ACKNOWLEDGMENT

This work has been partially supported through the following projects: S2013/MIT-2740 from Comunidad de Madrid, FIS2015-67367-C2-1-P and MAT2016-80394-R from the Spanish Ministry of Economy and Competitiveness. FCH, MM and FGR acknowledge CONICET and ANPCYT (Project PICT 2015-2285). XAFS experiments were partially supported by Projects XAFS2-20150061 and SXS-20150180 (LNLS, Campinas, Brazil).

REFERENCES

1. Murray, C. B.; Norris, D. J.; Bawendi, M. G. Synthesis and characterization of nearly monodisperse CdE (E = sulfur, selenium, tellurium) semiconductor nanocrystallites. *J. Am. Chem. Soc.* **1993**, *115*, 8706-8715.
2. Nam, J.; Won, N.; Bang, J.; Jin, H.; Park, J.; Jung, S.; Jung, S.; Park, Y.; Kim, S. Surface engineering of inorganic nanoparticles for imaging and therapy. *Adv. Drug Deliv. Rev* **2013**, *65*, 622-648.
3. Grim, J. Q.; Manna, L.; Moreels, I. A sustainable future for photonic colloidal nanocrystals. *Chem. Soc. Rev.* **2015**, *44*, 5897-5914.
4. Kovalenko, M. V.; Manna, L.; Cabot, A.; Hens, Z.; Talapin, D. V.; Kagan, C. R.; Klimov, V. I.; Rogach, A. L.; Reiss, P.; Milliron, D. J.; Guyot-Sionnnest, P.; Konstantatos, G.; Parak, W. J.; Hyeon, T.; Korgel, B. A.; Murray, C. B.; Heiss, W. Prospects of Nanoscience with Nanocrystals. *ACS Nano* **2015**, *9*, 1012-1057.
5. Rogach, A., *Semiconductor Nanocrystal Quantum Dots. Synthesis, Assembly, Spectroscopy and Applications*. Springer-Verlag Wien: 2008.
6. Aldakov, D.; Lefrancois, A.; Reiss, P. Ternary and quaternary metal chalcogenide nanocrystals: synthesis, properties and applications. *J. Mater. Chem. C* **2013**, *1*, 3756-3776.
7. Panda, S. K.; Hickey, S. G.; Waurisch, C.; Eychmuller, A. Gradated alloyed CdZnSe nanocrystals with high luminescence quantum yields and stability for optoelectronic and biological applications. *J. Mater. Chem.* **2011**, *21*, 11550-11555.
8. Cho, J.; Jung, Y. K.; Lee, J.-K. Kinetic studies on the formation of various II-VI semiconductor nanocrystals and synthesis of gradient alloy quantum dots emitting in the entire visible range. *J. Mater. Chem.* **2012**, *22*, 10827-10833.
9. Bailey, R. E.; Nie, S. Alloyed Semiconductor Quantum Dots: Tuning the Optical Properties without Changing the Particle Size. *J. Am. Chem. Soc.* **2003**, *125*, 7100-7106.
10. Donega, C. d. M. Synthesis and properties of colloidal heteronanocrystals. *Chem. Soc. Rev.* **2011**, *40*, 1512-1546.
11. Zhong, X.; Feng, Y.; Knoll, W.; Han, M. Alloyed ZnxCd1-xS Nanocrystals with Highly Narrow Luminescence Spectral Width. *J. Am. Chem. Soc.* **2003**, *125*, 13559-13563.
12. Sarma, D. D.; Nag, A.; Santra, P. K.; Kumar, A.; Sapra, S.; Mahadevan, P. Origin of the Enhanced Photoluminescence from Semiconductor CdSeS Nanocrystals. *J. Phys. Chem. Lett.* **2010**, *1*, 2149-2153.
13. Jang, E.; Jun, S.; Pu, L. High quality CdSeS nanocrystals synthesized by facile single injection process and their electroluminescence. *Chem. Commun.* **2003**, 0, 2964-2965.
14. Xie, R.; Kolb, U.; Li, J.; Basché, T.; Mews, A. Synthesis and Characterization of Highly Luminescent CdSe−Core CdS/Zn0.5Cd0.5S/ZnS Multishell Nanocrystals. *J. Am. Chem. Soc.* **2005**, *127*, 7480-7488.
15. Bae, W. K.; Kwak, J.; Park, J. W.; Char, K.; Lee, C.; Lee, S. Highly Efficient Green-Light-Emitting Diodes Based on CdSe@ZnS Quantum Dots with a Chemical-Composition Gradient. *Adv. Mater.* **2009**, *21*, 1690-1694.
16. Bae, W. K.; Char, K.; Hur, H.; Lee, S. Single-Step Synthesis of Quantum Dots with Chemical Composition Gradients. *Chem. Mater.* **2008**, *20*, 531-539.
17. Liu, F.-C.; Cheng, T.-L.; Shen, C.-C.; Tseng, W.-L.; Chiang, M. Y. Synthesis of Cysteine-Capped ZnxCd1-xSe Alloyed Quantum Dots Emitting in the Blue−Green Spectral Range. *Langmuir* **2008**, *24*, 2162-2167.
18. Qian, H.; Qiu, X.; Li, L.; Ren, J. Microwave-Assisted Aqueous Synthesis: A Rapid Approach to Prepare Highly Luminescent ZnSe(S) Alloyed Quantum Dots. *J. Phys. Chem. B* **2006**, *110*, 9034-9040.
19. Zhong, X.; Han, M.; Dong, Z.; White, T. J.; Knoll, W. Composition-Tunable ZnxCd1-xSe Nanocrystals with High Luminescence and Stability. *J. Am. Chem. Soc.* **2003**, *125*, 8589-8594.
20. Hyeokjin, L.; Holloway, P. H. Synthesis and characterization of colloidal ternary ZnCdSe semiconductor nanorods. *J. Chem. Phys.* **2006**, *125*, 164711-164711-7.
21. Beberwyck, B. J.; Surendranath, Y.; Alivisatos, A. P. Cation Exchange: A Versatile Tool for Nanomaterials Synthesis. *J. Phys. Chem. C* **2013**, *117*, 19759-19770.
22. Li, H.; Zanella, M.; Genovese, A.; Povia, M.; Falqui, A.; Giannini, C.; Manna, L. Sequential Cation Exchange in Nanocrystals: Preservation of Crystal Phase and Formation of Metastable Phases. *Nano Lett.* **2011**, *11*, 4964-4970.
23. Gupta, S.; Kershaw, S. V.; Rogach, A. L. 25th Anniversary Article: Ion Exchange in Colloidal Nanocrystals. *Adv. Mater.* **2013**, *25*, 6923-6944.
24. Rivest, J. B.; Jain, P. K. Cation exchange on the nanoscale: an emerging technique for new material synthesis, device fabrication, and chemical sensing. *Chem. Soc. Rev.* **2013**, *42*, 89-96.
25. Groeneveld, E.; Witteman, L.; Lefferts, M.; Ke, X.; Bals, S.; Van Tendeloo, G.; de Mello Donega, C. Tailoring ZnSe–CdSe Colloidal Quantum Dots via Cation Exchange: From Core/Shell to Alloy Nanocrystals. *ACS Nano* **2013**, *7*, 7913-7930.
26. Xia, X.; Liu, Z.; Du, G.; Li, Y.; Ma, M. Structural Evolution and Photoluminescence of Zinc-Blende CdSe-Based CdSe/ZnS Nanocrystals. *J. Phys. Chem. C* **2010**, *114*, 13414-13420.
27. Acebrón, M. a.; Galisteo-López, J. F.; Granados, D.; López-Ogalla, J.; Gallego, J. M.; Otero, R.; López, C.; Juárez, B. H. Protective Ligand Shells for Luminescent SiO2-Coated Alloyed Semiconductor Nanocrystals. *ACS Appl. Mater. Interfaces* **2015**, *7*, 6935-6945.
28. van Driel, A. F.; Allan, G.; Delerue, C.; Lodahl, P.; Vos, W. L.; Vanmaekelbergh, D. Frequency-Dependent Spontaneous Emission Rate from CdSe and CdTe Nanocrystals: Influence of Dark States. *Phys. Rev. Lett.* **2005**, *95*, 236804-236804-4.
29. Gong, K.; Zeng, Y.; Kelley, D. F. Extinction Coefficients, Oscillator Strengths, and Radiative Lifetimes of CdSe, CdTe, and CdTe/CdSe Nanocrystals. *J. Phys. Chem. C* **2013**, *117*, 20268-20279.
30. Garrett, M. D.; Dukes Iii, A. D.; McBride, J. R.; Smith, N. J.; Pennycook, S. J.; Rosenthal, S. J. Band Edge Recombination in CdSe, CdS and CdSxSe1−x Alloy Nanocrystals Observed by Ultrafast Fluorescence Upconversion: The Effect of Surface Trap States. *J. Phys. Chem. C* **2008**, *112*, 12736-12746.
31. Islam, R.; Rao, D. R. X-ray photoelectron spectroscopy of Zn1−xCdxSe thin films. *J. Electron Spectros. Relat. Phenomena* **1996**, *81*, 69-77.
32. Park, J. J.; Lacerda, S. H. D. P.; Stanley, S. K.; Vogel, B. M.; Kim, S.; Douglas, J. F.; Raghavan, D.; Karim, A. Langmuir Adsorption

Study of the Interaction of CdSe/ZnS Quantum Dots with Model Substrates: Influence of Substrate Surface Chemistry and pH. *Langmuir* **2009**, *25*, 443-450.

33. XPS simplified, XPS interpretation of Zn. https://xpssimplified.com/elements/zinc.php.

34. Lauermann, I.; Bär, M.; Fischer, C.-H. Synchrotron-based spectroscopy for the characterization of surfaces and interfaces in chalcopyrite thin-film solar cells. *Sol. Energ. Mat. Sol. C.* **2011**, *95*, 1495-1508.

35. Wang, G.; Li, Z.; Li, M.; Chen, C.; Lv, S.; Liao, J. Aqueous Phase Synthesis and Enhanced Field Emission Properties of ZnO-Sulfide Heterojunction Nanowires. *Sci. Rep.* **2016**, *6*, 29470-29470-9.

36. Santra, P. K.; Viswanatha, R.; Daniels, S. M.; Pickett, N. L.; Smith, J. M.; O'Brien, P.; Sarma, D. D. Investigation of the Internal Heterostructure of Highly Luminescent Quantum Dot−Quantum Well Nanocrystals. *J. Am. Chem. Soc.* **2009**, *131*, 470-477.

37. Wang, G.; Huang, B.; Li, Z.; Lou, Z.; Wang, Z.; Dai, Y.; Whangbo, M.-H. Synthesis and characterization of ZnS with controlled amount of S vacancies for photocatalytic H2 production under visible light. *Sci. Rep.* **2015**, *5*, 8544-8544-7.

38. Mukherjee, S.; Hazarika, A.; Santra, P. K.; Abdelhady, A. L.; Malik, M. A.; Gorgoi, M.; O'Brien, P.; Karis, O.; Sarma, D. D. Determination of Internal Structures of Heterogeneous Nanocrystals Using Variable-Energy Photoemission Spectroscopy. *J. Phys. Chem. C* **2014**, *118*, 15534-15540.

39. Yiu, Y. M.; Murphy, M. W.; Liu, L.; Hu, Y.; Sham, T. K. Experimental and theoretical XANES of CdS_xSe_{1-x} nanostructures. *AIP Conference Proceedings* **2014**, *1590*, 26-31.

40. Van der Snickt, G.; Dik, J.; Cotte, M.; Janssens, K.; Jaroszewicz, J.; De Nolf, W.; Groenewegen, J.; Van der Loeff, L. Characterization of a Degraded Cadmium Yellow (CdS) Pigment in an Oil Painting by Means of Synchrotron Radiation Based X-ray Techniques. *Anal. Chem.* **2009**, *81*, 2600-2610.

41. Corrias, A.; Conca, E.; Cibin, G.; Mountjoy, G.; Gianolio, D.; De Donato, F.; Manna, L.; Casula, M. F. Insights into the Structure of Dot@Rod and Dot@Octapod CdSe@CdS Heterostructures. *J. Phys. Chem. C* **2015**, *119*, 16338-16348.

42. Loglio, F.; Telford, A. M.; Salvietti, E.; Innocenti, M.; Pezzatini, G.; Cammelli, S.; D'Acapito, F.; Felici, R.; Pozzi, A.; Foresti, M. L. Ternary CdxZn1−xSe deposited on Ag (111) by ECALE: Electrochemical and EXAFS characterization. *Electrochim. Acta.* **2008**, *53*, 6978-6987.

43. Valeev, R. G.; Romanov, E. A.; Vorobiev, V. L.; Mukhgalin, V. V.; Kriventsov, V. V.; Chukavin, A. I.; Robouch, B. V. Structure and properties of ZnS x Se 1− x thin films deposited by thermal evaporation of ZnS and ZnSe powder mixtures. *Mater. Res. Express* **2015**, *2*, 025006.